Experimental Determination of Dominant Scattering Mechanisms in Scaled InAsSb Quantum Well

A. Agrawal[1], A. Ali[1], R. Misra[2], P. E. Schiffer[2], B. R. Bennett[3] , J. B. Boos[3] and S. Datta[1]
[1]Department of Electrical Engineering, The Pennsylvania State University, University Park, PA 16802, USA
[2]Department of Physics, The Pennsylvania State University, University Park, PA 16802, USA
[3]Naval Research Laboratory, Washington, DC 20375, USA

Antimonide based compound semiconductors have gained considerable interest in recent years due to their superior electron and hole transport properties [1]. A Mixed anion $InAs_ySb_{1-y}$ quantum well heterostructure with high electron mobility of 13,300 cm^2/Vs has already been demonstrated at a sheet carrier density of $2x10^{12}$ $/cm^2$, albeit for a thick EOT quantum well (QW) structure [2]. A thin EOT structure is desired for improving short channel effects while maintaining the high electron mobility in the QW. In this paper, we study the low field electron transport properties in the high mobility $InAs_{0.8}Sb_{0.2}$ quantum well as we scale the QW heterostructure. Fig. 1(a),(b) show the schematic of the thick (T_{QW}=12nm) and scaled (T_{QW}=7.5nm) quantum well FET structure using $InAs_{0.8}Sb_{0.2}$ as channel material, $In_{0.2}Al_{0.8}Sb$ barrier layer and an ultra-thin GaSb surface layer for avoiding surface oxidation of Al in the barrier [2]. Fig. 2(a),(b) show the simulated energy band diagram of the two structures using self-consistent Schrodinger-Poisson simulation, indicating strong electron confinement in the QW. The effect of nonparabolicity on thick QW with T_{QW}=12nm has already been studied and an effective mass (m^*) of $0.043m_0$ has been extracted experimentally [3]. For scaled QW the subband spacing was adjusted in order to achieve electron sheet charge density as a function of temperature, and the extracted density of states $m^*=0.05m_0$ was correlated to the transport effective mass. Experimental work to verify the obtained effective mass for scaled QW is underway.

Hall measurements were performed on the device layers by varying the temperature from 4K-300K. We extract the dominant scattering mechanisms that are responsible for limiting the mobility at low and high temperatures. The relaxation time approximation (RTA) applied to the Boltzmann transport equation is the theoretical framework employed to estimate the scattering rates. The scattering of the electrons confined in the quantum-well consists of a variety of mechanisms having unique temperature dependence which explain the overall mobility characteristics of the fabricated heterostructure. The inverse of the total relaxation time, τ_{tot} , can be calculated from the sum of the scattering rates for the individual scattering processes. There are six scattering mechanisms limiting the electron mobility: acoustic deformation potential scattering, polar optical phonon scattering, remote ionized impurity scattering, alloy disorder scattering, interface roughness scattering, and coulomb scattering due to charge trapped at the barrier and channel interface (Tamm States) [4]. The scattering rates are finally derived using the Fermi's golden rule.

Fig. 3 shows experimental and modeled sheet carrier concentration as a function of temperature in the channel. The significant contribution from second subband mandates the inclusion of intersubband scattering along with intrasubband scattering. Fig. 4 shows the experimental and modeled hall mobility vs temperature for electrons in the InAsSb channel, indicating the dominant scattering mechanisms at various temperatures. For 12nm thick quantum well, interface charge scattering from Tamm States is the primary source for limiting mobility at both room temperature and low temperature. In the case of scaled quantum well of 7.5nm thickness and 5nm thick barrier, the remote ionized impurity scattering increases by 3x due to reduction in spacer layer thickness, and interface roughness scattering increases by 75x because electrons are closer to the interface and the perturbation in potential is much stronger than that in thick quantum well. Table I lists the parameter values used for scattering calculation for mobility analysis using RTA.

Fig. 5 and 6 show transfer and output characteristics for the thick and scaled MOS-QWFET at room temperature depicting enhancement mode operation for the scaled device. Excellent performance with an I_{ON}/I_{OFF} = 700 over 1V V_{GS} swing is obtained for QW with T_{QW}=7.5nm. Fig. 7 shows the pareto plot indicating % contribution of different scattering components to total mobility at 300K for thick and scaled QW. This provides a clear picture regarding the detrimental scattering mechanisms in each device.

In conclusion, high electron Hall mobility of 13,300 cm^2/Vs at Ns=$2x10^{12}$ $/cm^2$ is achieved on the fabricated $InAs_{0.8}Sb_{0.2}$ QW FET device with 12nm thick QW and 5,500 cm^2/Vs at Ns=$1.7x10^{12}$ $/cm^2$ is obtained on scaled QWFET with 7.5nm QW thickness. Excellent agreement between experimental and modeled results for a wide range of temperature has been obtained.

[1] B. R. Bennett, et. al., *Journal of Crystal Growth*, Vol. 312, pp.37 (2009), [2] A. Ali et. al., *Electron Devices Meeting (IEDM)*, pp.6.3.1-6.3.4, Dec. 2010 , [3] A. Ali et. al., *IEEE TED*, doi: 10.1109/TED.2011.2110652 [4] H. Kroemer et.al., *J. Vac. Sci. Technol. B*, 10(4), pp.1769, Jul/Aug 1992

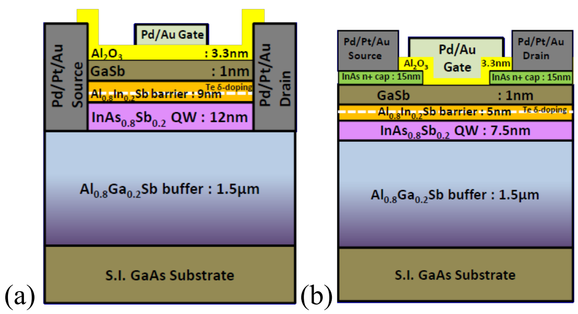

Fig. 1(a) Schematic of the $InAs_{0.8}Sb_{0.2}$ MOS-QWFET on GaAs substrate with 12nm QW thickness and 9nm barrier layer (b) Schematic of scaled $InAs_{0.8}Sb_{0.2}$ MOS QWFET with 7.5nm QW thickness and 5nm barrier layer

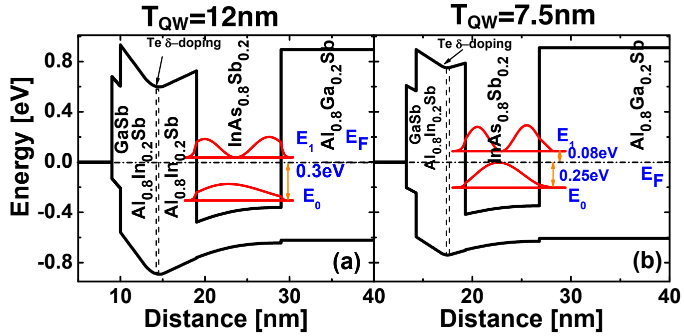

Fig. 2 Band diagram of $InAs_{0.8}Sb_{0.2}$ QW heterostructure with 12nm and 7.5nm QW thickness and 1nm GaSb layer from Schrodinger-Poisson simulation indicating strong electron confinement.

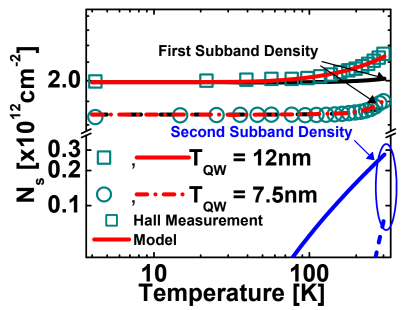

Fig. 3 Experimental and modeled sheet charge density vs temperature in $InAs_{0.8}Sb_{0.2}$ channel for 12nm and 7.5nm QW thickness. The contribution from first and second subband is indicated.

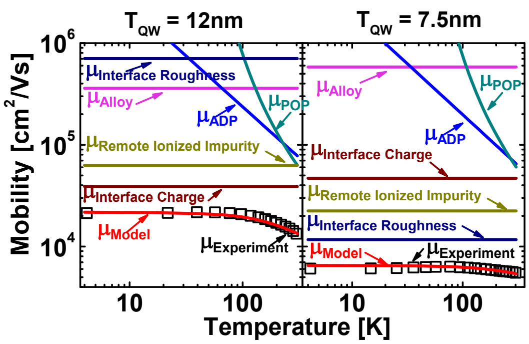

Fig. 4 Experimental and modeled electron mobility in $InAs_{0.8}Sb_{0.2}$ QW channel of 12nm and 7.5nm thickness, depicting dominant scattering mechanisms at low and room temperature.

Parameter	Value
Acoustic Deformation Potential	4.8 eV
Polar Optical Phonon Energy	27.8 meV
Alloy Disorder Potential	0.3eV
Interface Charge	$6x10^{11}$ /cm^2
Mean height of Roughness	6.2Å(T_{QW}=12nm), 6.8Å(T_{QW}=7.5nm)
Correlation Length	20nm
Remote Ionized Impurity	$1.8x10^{12}$ /cm^2

Table I. Values of different parameters used for scattering rate calculation using Relaxation Time Approximation.

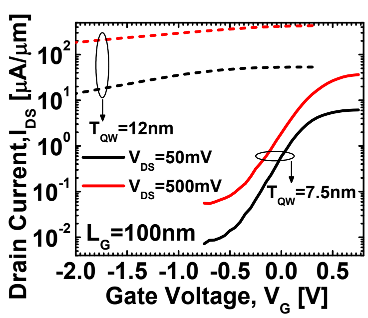

Fig. 5 Drain current(I_D) and gate current(I_G) vs. gate voltage(V_G) of the two $InAs_{0.8}Sb_{0.2}$ MOS-QWFET with QW thickness=7.5nm and 12nm. Scaled QWFET shows superior enhancement mode characteristics than thick QWFET.

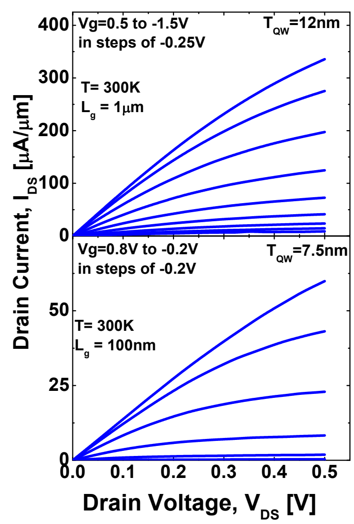

Fig. 6 I_D vs. V_{DS} of $InAs_{0.8}Sb_{0.2}$ MOS-QWFET with QW thickness=7.5nm and 12nm and Al_2O_3-GaSb composite stack at 300K.

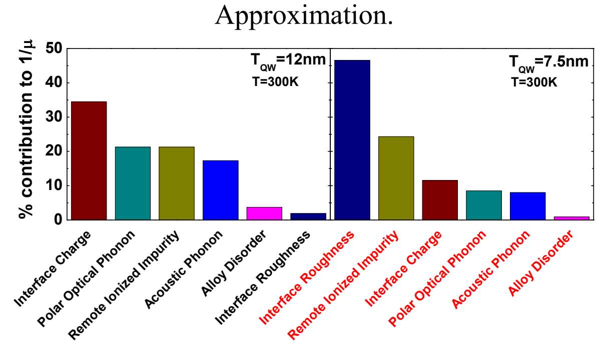

Fig. 7 Pareto plot showing %contribution of different scattering mechanisms to total mobility at 300K for thick and scaled QW. Interface charge scattering dominates for T_{QW}=12nm and interface roughness scattering dominates for T_{QW}=7.5nm.